

The real pendulum: theory, simulation, experiment



Giacomo Torzo^{1,2}, Paolo Peranzoni³

¹Department of Physics, Padova University, via Marzolo 8, 35131, Italy.

²ICIS-CNR, Corso Stati Uniti 24, Padova, Italy.

³Liceo Alvisè Cornaro, via Riccoboni 14, Padova, Italy.

E-mail: torzo@padova.infm.it

(Received 10 February 2009; accepted 30 April 2009)

Abstract

We propose a new tool for laboratory curricula based on computer-aided data acquisition and analysis. A pendulum coupled to a low-friction rotary sensor offers variable length, variable mass, variable oscillation plane (to change the effective gravitational restoring torque) and two different kind of damping torque: “dynamic friction” (almost constant) and “viscous” proportional to the angular velocity. Simple models implemented in common spreadsheets allow to compare the experimental results with the theoretical predictions.

Keywords: Data Handling and Computation, Mechanical Instruments and Measurement Methods, Friction.

Resumen

Proponemos una nueva herramienta para el programa de estudio del laboratorio basado en la adquisición de datos y análisis asistido por computadora. Un péndulo acoplado a un sensor rotatorio de baja fricción ofrece longitud variable, masa variable, plano de oscilación variable (para cambiar la torca de restauración efectiva) y dos tipos de torca amortiguada: “fricción dinámica” (casi constante) y “viscosa” proporcional a la velocidad angular. Modelos simples implementados en hojas de cálculo comunes permiten el comparar los resultados experimentales con las predicciones teóricas.

Palabras clave: Manipulación de Datos y Computación, Instrumentos Mecánicos y métodos de medición, Fricción.

PACS: 06.50, 07.10, 46.30P

ISSN 1870-9095

I. NUMERICAL SIMULATION IN PHYSICS

It is well known that scientific research consists in a dialectic process, oscillating between theory and experiment, frequently including as an intermediate step a numerical simulation of phenomena, but it is not easy to reproduce this whole process at school. In particular some teacher assumes the numerical simulation as a *substitution* of the experiment in the lab. This may be misleading: in fact simulation and experiment are not at all equivalent. The results of simulations are completely determined by the underlying modelization, while the results of real experiments are mostly determined by the physical phenomena, even when the experimental setup (usually inspired by the model present in the researcher mind) takes an important role.

Classic physics frequently needs using differential equations, which are rarely included in high school curricula. As a consequence, the teacher often restricts his teaching to very simple phenomena, or he (she) tries tricks and turnarounds, or gives to students bare formulas justified by sentences as “... it may be prove that...”. A

better choice allowed by the widespread of personal computers both at school and at home, is the use of numerical integration of differential equations. This approach may be made quite simple by using iterated computation in a common spreadsheet (*e.g.* Microsoft Excel).

The working principle of this method may be easily explained: for example if we want to integrate the motion equation in one dimension, given the initial conditions of a body (position x_0 and velocity v_0 at the time t_0), we may linearly approximate the same quantities after a short time interval Δt by the equations

$$v(t_0 + \Delta t) = v(t_0) + a_m \Delta t, \quad (1)$$

and

$$s(t_0 + \Delta t) = s(t_0) + v_m \Delta t, \quad (2)$$

where we assume a constant acceleration equal to the mean value $a_m = [v(t + \Delta t) - v(t)] / \Delta t$ in the time interval Δt ,

and a constant velocity v_m equal to the mean value $v_m = [s(t + \Delta t) - s(t)] / \Delta t$.

Repeating the process for the next time interval we obtain the calculated vales for $t=t_o+2 \Delta t$ and then for $t=t_o+3 \Delta t...$ and so on.

There is one difficulty: the described procedure assumes we know the *mean* value of acceleration, while we know only the *initial* value. One solution (firstly suggested by Richard Feynman) is to use the *initial acceleration* to calculate the velocity at the time $t_o + \Delta t/2$, and to take this value as *mean value of the velocity* in the interval Δt , and then to proceed with the recursive calculations that give positions at times $\Delta t, 2\Delta t, 3\Delta t, \dots$ and velocities at the times $\Delta t + \Delta t/2, 2\Delta t + \Delta t/2, 3\Delta t + \Delta t/2, \dots$

In order to simplify the procedure to be implemented in the electronic spreadsheet, we may use the *initial acceleration* to calculate the next velocity and the *final velocity* to calculate the next position.

This approach may become particularly useful when dealing with phenomena that are intrinsically *non-linear*, as for example the pendulum oscillations at large amplitudes.

II. THE PENDULUM MOTION EQUATION

Let us consider a pendulum consisting of a uniform thin rod of length l and mass m rotating about a fixed pivot located at one of its end. The rod is attached to a uniform disc of mass m' and radius r centred on the pivot and damped by a resistant torque T_R . A point-like mass M is fixed on the rod at the distance L from the pivot.

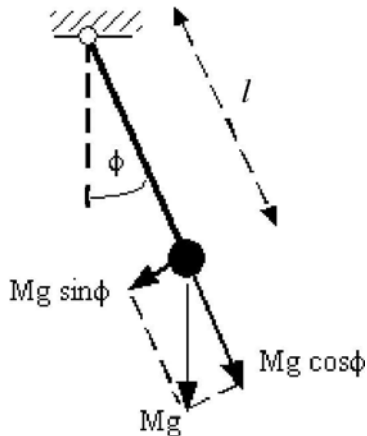


FIGURE 1. Sketch of forces for the ideal pendulum.

The motion equation may be obtained by equating the time derivative of the angular momentum $I \partial \omega / \partial t$ to the net torque $T = -(ml/2 + ML) g \sin \phi + T_R(\omega)$:

$$I \partial^2 \phi / \partial t^2 = -(ml/2 + ML)g \sin \phi + T_R(\omega), \quad (3)$$

where ϕ is the elongation, $\omega = \partial \phi / \partial t$ is the angular velocity, $I = 1/3 ml^2 + ML^2 + 2/3 m' r^2$ is the momentum of inertia, and $T_R(\omega)$ is the resistant torque whose value depends on the kind of damping mechanism.

The equation may be simplified into the form:

$$\partial^2 \phi / \partial t^2 = -g(\zeta/L) \sin \phi + T_R(\omega)/I, \quad (4)$$

where the coefficient ζ accounts for the pendulum non-ideality (due to the masses of the rod and of the disc):

$$\zeta = \left(1 + \frac{1}{2} \frac{ml}{ML}\right) \left(1 + \frac{1}{3} \frac{ml^2}{ML^2} + \frac{2}{3} \frac{m'r^2}{ML^2}\right).$$

For $l \approx L$, $r \ll l$, and $m \ll M$ we get $\zeta \approx 1$, and the equation becomes the equation for *ideal pendulum* with damping:

$$\partial^2 \phi / \partial t^2 = -(g/L) \sin \phi + T_R(\omega)/I. \quad (5)$$

For small oscillation amplitudes, by letting $\sin \phi \approx \phi$, Eq. (5) may be approximated as:

$$\partial^2 \phi / \partial t^2 = -(g/L)\phi + T_R(\omega)/I. \quad (6)$$

This, for $T_R = 0$ (no damping), becomes

$$\partial^2 \phi / \partial t^2 = -(g/L)\phi, \quad (7)$$

which has the stationary harmonic solution with angular velocity $\omega = \sqrt{g/L}$ and period $T = 2\pi \sqrt{L/g}$.

III. THE NUMERICAL SIMULATION

Solving the simple equation (7) using calculus is often a too difficult task for students in high schools. Much easier is to find numerical solutions: with the previously described method the students may graph excellent approximated solutions not only for the simple equation (7) but also for the more difficult Eq. (6) (damped oscillations) and even for Eq. (5) (anharmonic oscillations).

Let us start with the case of undamped motion for large oscillation amplitude, *i.e.* assuming $T_R = 0$, while keeping the *non-linear* term of Eq. (5). The angular acceleration is $d^2 \phi(t) / dt^2 = \alpha(t) = [g/L] \sin \phi(t)$.

The relations to be used in the numerical computation are therefore:

$$\alpha(t) = [g/L] \sin \phi(t), \quad (8)$$

$$\omega(t + \Delta t) = \omega(t) + \alpha(t) \Delta t, \quad (9)$$

$$\phi(t + \Delta t) = \phi(t) + \omega(t + \Delta t) \Delta t, \quad (10)$$

where we remark that in Eq. (10) the angular position is calculated using the *final* value of the angular velocity in the time interval Δt , while the angular velocity is calculated in Eq.(9) using the *initial* value of the angular acceleration.

Figure 2 shows the three plots of angle, velocity and acceleration versus time at large amplitude oscillations (90°).

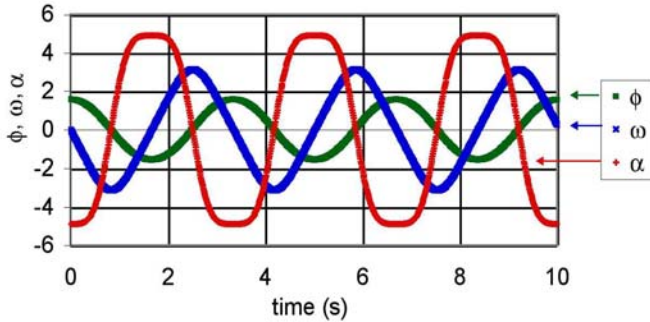


FIGURE 2. Angle, velocity and acceleration versus time for undamped pendulum al large amplitude oscillations.

It may be noted that the motion is strongly anharmonic: while the angle graph seems to be sinusoidal, the velocity graph approaches a triangular wave and the acceleration graph approaches a squarewave...

From the data obtained in the spreadsheet recursive calculations we may easily compare the behavior of the real acceleration with the harmonic approximation (figure 3) obtained by substituting in Eq. (4) the term $[g/L]\sin\phi(t)$ with its linear approximation $[g/L]\phi(t)$.

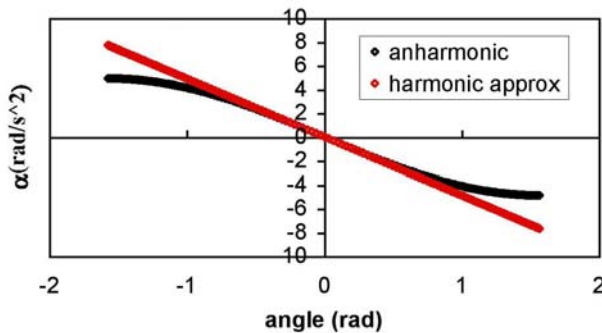


FIGURE 3. Comparison between real and approximated acceleration

IV. THE PENDULUM MOTION WITH DAMPING

If we introduce damping into our model the acceleration in Eq. (8) becomes:

$$\alpha(t) = -(g/L) \sin\phi(t) - \text{sgn}(\omega)\alpha_f(t), \quad (11)$$

where α_f is the acceleration due to friction, whose sign is always opposite to the sign of the velocity ω .

The friction force however may depend on velocity in different ways: it may be almost *constant* (sliding friction) or proportional to the velocity (viscous friction)

In the first case we have:

$$\alpha(t) = -(g/L) \sin\phi(t) - A \text{sgn}[\omega(t)], \quad (12)$$

where A is a constant.

In the second case we have:

$$\alpha(t) = -(g/L) \sin\phi(t) - C\omega(t), \quad (13)$$

where C is another constant.

The above mentioned assumptions for the friction forces lead to some predictions about the pendulum motion. Let us briefly discuss the two different cases [1].

A. Sliding friction

Assuming a *constant* friction torque with negative sign with respect to the sign of the angular velocity $\omega = d\phi/dt$, we get $T_R = +C$ for $\omega > 0$, $T_R = -C$ for $\omega < 0$ and $T_R = 0$ for $\omega = 0$, i.e. $T_R = C \text{sgn}(\omega)$, and the motion equation becomes:

$$\partial^2\phi/\partial t^2 = -(g/L)\phi - (C/I)\text{sgn}\partial\phi/\partial t. \quad (14)$$

Let us analyze small oscillations starting from initial elongation ϕ_0 from rest ($\omega_0 = 0$).

During the first half-oscillation the pendulum will sweep the total angle $\phi_0 + \phi_1$, and it will reach a situation ($\phi = \phi_1$, $\omega = 0$) where we may calculate the energy balance.

The initial potential energy $MLg(1 - \cos\phi_0)$ equals the new potential energy $MLg(1 - \cos\phi_1)$ plus the energy lost due to the dry friction work $C(\phi_0 + \phi_1)$, or:

$$MLg(\cos\phi_0 - \cos\phi_1) = C(\phi_0 + \phi_1). \quad (15)$$

By using the Werner formula, we have:

$$\cos\phi_0 - \cos\phi_1 = 2 \sin\left[\frac{(\phi_0 + \phi_1)}{2}\right] \sin\left[\frac{(\phi_0 - \phi_1)}{2}\right], \quad (16)$$

and using again the approximation $\sin\phi \approx \phi$:

$$\cos\phi_0 - \cos\phi_1 = (\phi_0 + \phi_1)(\phi_0 - \phi_1)/2, \quad (17)$$

and the energy balance equation (15) gives for the elongation decrement $\Delta\phi = (\phi_0 - \phi_1)$ during one half-period:

$$\Delta\phi = 2C/MLg. \quad (18)$$

The calculation may be repeated for the second half-period, leading to the same result. As a conclusion: the elongation, during each half-period, decreases by the constant value $\Delta\phi=2C/MLg$.

Relation (18) gives an evaluation of the friction torque $C = MLg \Delta\phi/2$, where the decrement $\Delta\phi$ is expressed in rad.

B. Viscous damping

Let us now analyze the case of *viscous damping*, (torque proportional to the angular velocity). The motion equation is now:

$$\partial^2\phi / \partial t^2 = -(g/L)\phi - (\gamma/I)\partial\phi / \partial t, \quad (19)$$

and, with the positions $\delta = \gamma/2I$ and $\omega_0^2 = g/L$, it becomes

$$\partial^2\phi / \partial t^2 + 2\delta\phi / \partial t + \omega_0^2\phi = 0. \quad (20)$$

This equation, for small damping ($\delta \ll \omega_0$), has the analytical solution $\phi(t) = \phi_0 e^{-\delta t} \cos \omega t$, where $\omega = \sqrt{\omega_0^2 - \delta^2} \approx \omega_0$

The elongation amplitude should therefore decrease exponentially, i.e. the decrement during each half-period should decrease proportionally to the amplitude itself.

V. NUMERICAL SIMULATIONS

The previous analysis should give to students a picture of the predicted pendulum motion for the two cases, but a graph of the motion would be much more useful. Numerical simulation offer an easy way to obtain such graphs (figures 4 and 5).

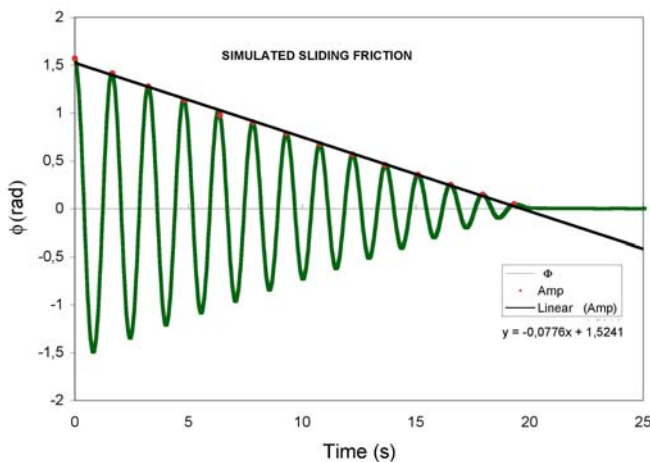


FIGURE 4. Numerical simulation of oscillations damped by sliding friction.

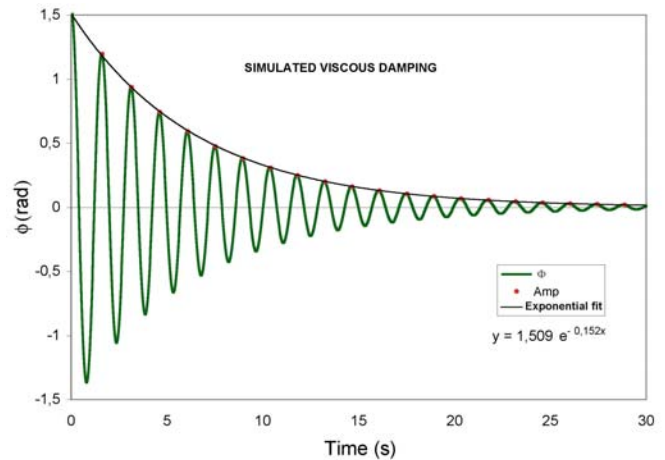


FIGURE 5. Numerical simulation of oscillations damped by viscous friction.

VI. EXPERIMENTAL RESULTS

The theoretical models and numerical simulation may be compared with experimental results by using a device which exploits a real-time data acquisition system to obtain a complete record of the motion (computer assisted **Real Time Laboratory**).

Our pendulum is made of a perforated rubber ball (approximating a point-mass) attached to a thin aluminium rod (a knitting needle) whose end is fixed to the rotary sensor axis (figure 6).

The pendulum effective length can be varied by sliding the rubber ball along the rod. The mass may be changed by using rubber balls of different sizes.

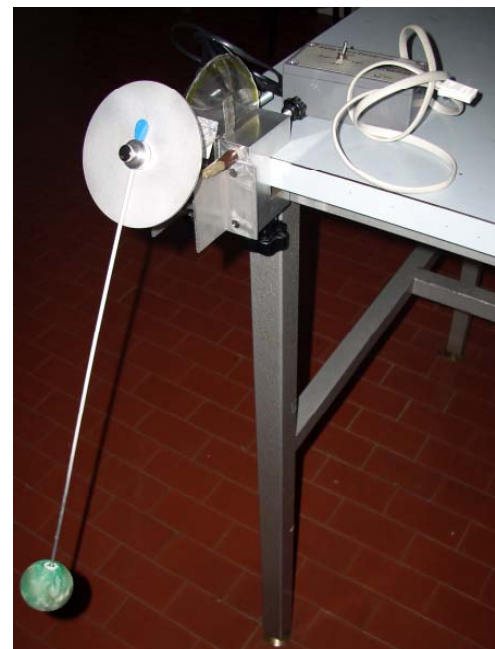


FIGURE 6. The RTL pendulum.

The angular deviation from horizontal position of the pendulum's rotation axis can also be varied, and measured by a goniometer mounted close to the encoder. This feature allows to simulate the pendulum motion in a reduced gravity acceleration, as shown later in section IX.

When the rotation axis is horizontal, the oscillation may be damped by two kinds of resistant torque T_R : 1) a *viscous drag* provided by a magnet placed close to an aluminium disc fixed to the rotary sensor axis (the Foucault currents due to the magnet-disc interaction produce a torque proportional to the angular velocity of the disc), or 2) a nearly constant torque (*sliding friction*) provided by a small brush sweeping the disc.

The intensity of each resistant torque may be varied by adjusting the position (of either the magnet or the brush) with respect to the disc.

The RTL data acquisition system exploits a home-made rotary sensor with low-friction optical encoder [3], connected to a Texas Instrument graphing calculator through CBL interface (or to a PC through a LabPro interface) [4].

The rotary encoder allows recording the elongation ϕ versus time. From the measured values we may calculate and graph the absolute values of ϕ , and use them to build a new plot of the peak values of ϕ (amplitude) versus time.

A. Sliding friction

In figure 7 we report two records of the oscillations (obtained with a pendulum length $l = 0.5$ m, a mass $M = 30$ g) for two values of the friction torque.

The expected linear dependence of the amplitude on time is apparent. The last oscillations in both graphs indicate that the damping decreases at very small elongations: this is due to the brush bristles elasticity that kills the sliding friction (when the disc motion is small, the bristles bend and their free end follows the disc rotation: the point contact is fixed on disc and no sliding occurs).

The values of the slope, in the linear fit of amplitude vs. time, are -3 degrees/s and -6.5 degrees/s, respectively. With a period given approximately by $T = 2\pi\sqrt{L/g} = 1.42$ s we may calculate in both cases the value of $\Delta\phi$, and we obtain for the friction torque $C = MLg \Delta\phi/2$ the two values $C = 5$ mJ and $C = 12$ mJ, respectively.

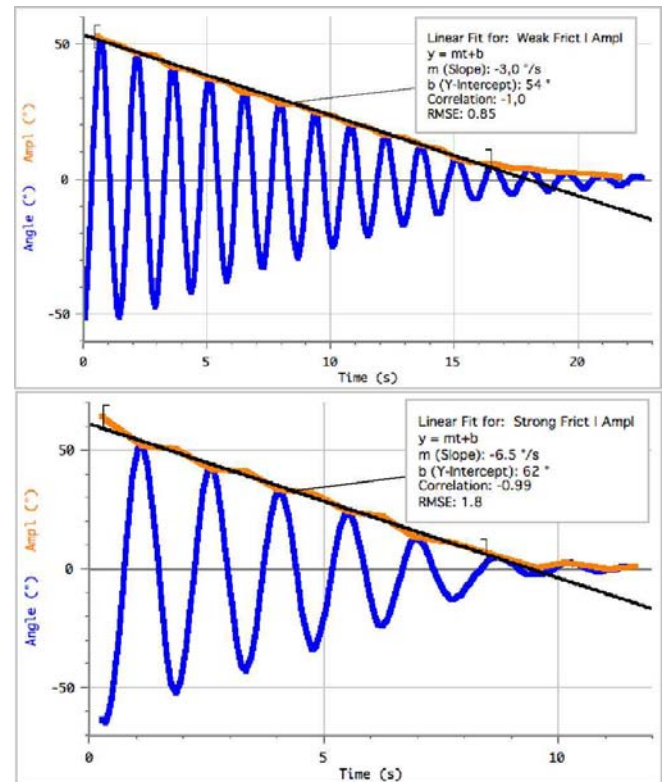


FIGURE 7. Oscillations recorded with different values of the dry friction.

B. Viscous damping

The same procedure may be used to analyze the motion in case of viscous drag, due to the magnet-disc interaction. In figure 8 we report the graphs of elongation vs. time and exponential best fits to the curves of amplitude vs. time, for two values of magnet-disc distance (1.5 mm and 1 mm, respectively). The fitting curve is $\phi(t) = \phi_0 \exp(-\delta t) + \phi_1$, where the damping coefficient δ is the reciprocal of the decay constant τ . Reducing the magnet-disc gap decreases the time constant from 33 seconds to 14 seconds.

Equivalent plots on the right side of figure 8 show the logarithm of amplitude decreasing linearly with time.

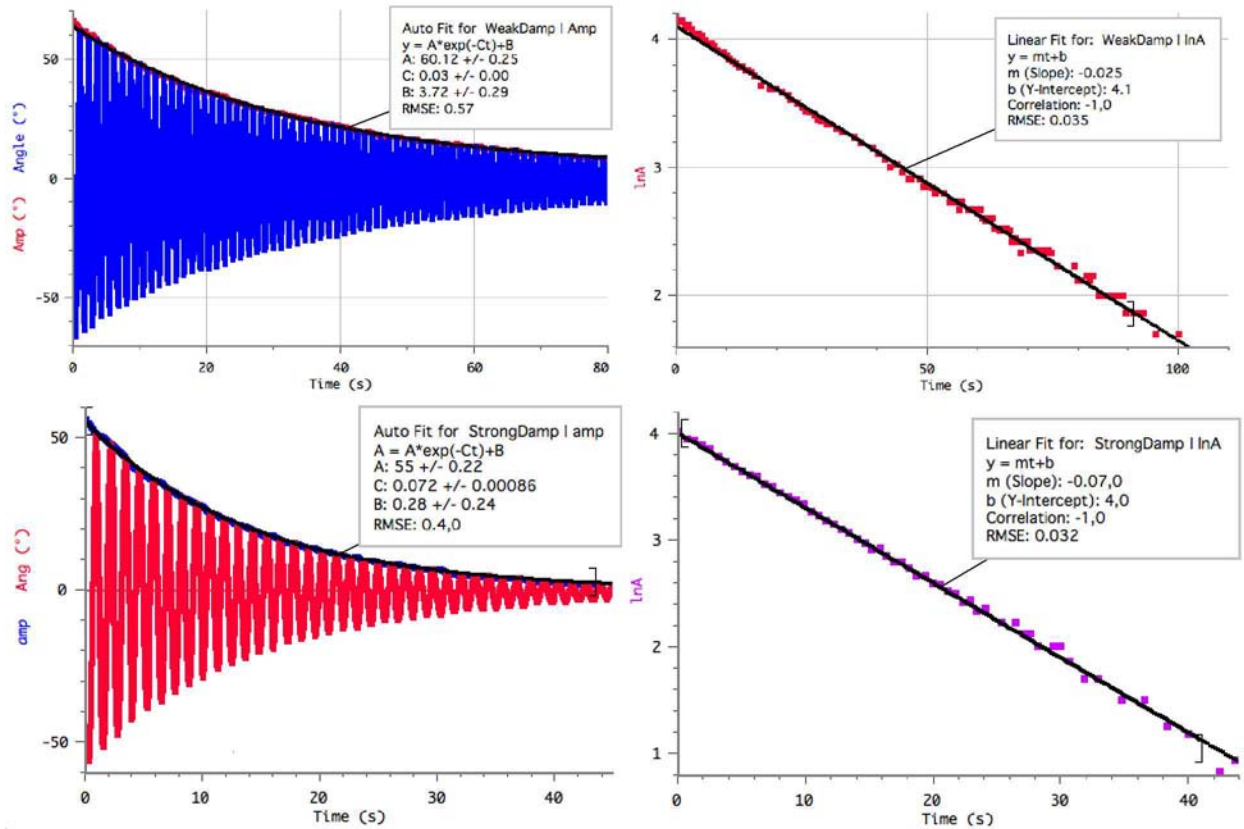


FIGURE 8. Oscillations recorded with different values of the viscous damping: the amplitude vs. time is fitted by an exponential function at left . A linear regression of the natural log of amplitude vs. time is shown at right.

X. COMPARING EXPERIMENTAL RESULTS WITH SIMULATIONS

The RTL technique allows an easy comparison between experimental results and numerical simulations because data are taken by sampling angles ϕ at equal time intervals Δt . Angular velocity and acceleration are then calculated in real time as $\omega = [\phi(t + \Delta t) - \phi(t)] / \Delta t$, $\alpha = [\omega(t + \Delta t) - \omega(t)] / \Delta t$.

An example of comparison is presented in figure 9 for sliding friction: initial values and friction coefficient are properly adjusted to fit the experimental data. The final part of the experimental graph indicates that the damping decreases at small elongations: this is due to the brush bristles elasticity that reduces the sliding friction at slow disc motion (the bristles bend and their free end follows the disc rotation: the point contact is fixed on disc and no sliding occurs).

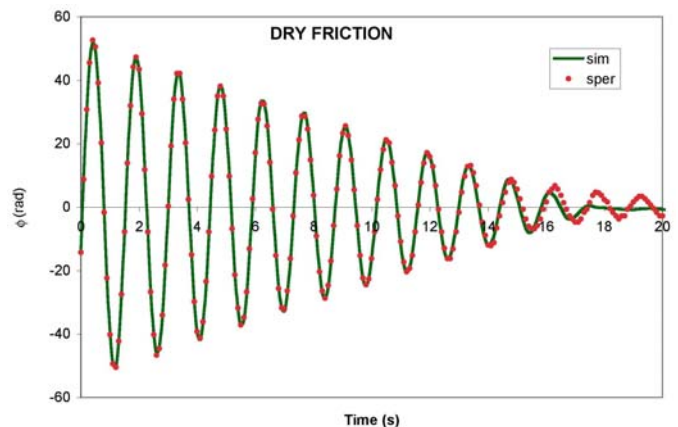


FIGURE 9. The line represents the values calculated by numerical simulation with the dry friction model using $(2\delta=0.3 \text{ rad/s}^2)$, and the dots are the measured values.

A similar comparison for the case of viscous friction is shown in figure 10.

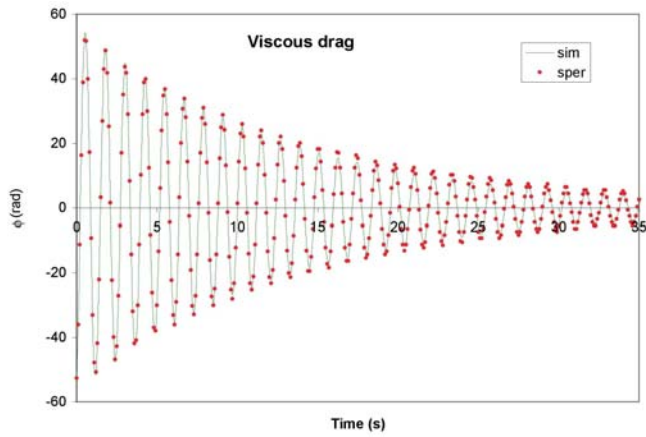


FIGURE 10. The line represents the values calculated by numerical simulation with the viscous friction model using $2\delta = 0.153 \text{ s}^{-1}$, and the dots are the measured values.

In both cases the agreement between experimental data and numerical simulation is extremely good.

IX. PENDULUM WITH TILTED ROTATION AXIS

When the pendulum rotation axis is tilted by an angle β , with respect to the usual horizontal position, the component g' of the gravitational force acting on the mass M which produces the driving torque is reduced by the factor $\cos \beta$.

Therefore the harmonic solution of the motion equation will predict a reduced angular velocity $\omega = \sqrt{g'/L} = \sqrt{g \cos \beta / L}$ and an increased period $T' = 2\pi \sqrt{L/g \cos \beta}$.

TABLE I. The predicted and measured values of the period for different tilt angles.

Angle β (degrees)	$(\cos \beta)^{1/2}$	T (s)	T' (s)
0	0.000	1.41	1.41
5	0.997	1.41	1.40
10	0.99	1.42	1.41
15	0.98	1.44	1.42
20	0.96	1.47	1.44
25	0.95	1.48	1.45
30	0.93	1.51	1.48
35	0.90	1.56	1.52
40	0.87	1.62	1.57
45	0.84	1.68	1.61
50	0.80	1.76	1.68
55	0.75	1.88	1.79
60	0.70	2.01	1.85

In Table I we report a comparison between the predicted and measured values for the period for different values of the tilt angle β . The same data are graphically shown in figures 11 and 12.

The real pendulum: theory, simulation, experiment

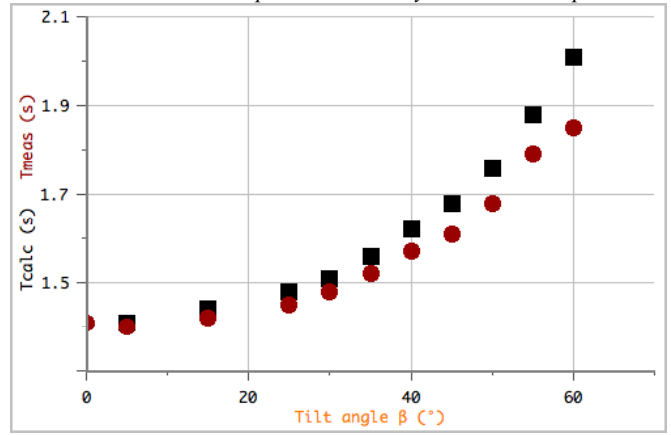


FIGURE 11. Calculated (squares) and measured (circles) periods vs. the tilt angle β .

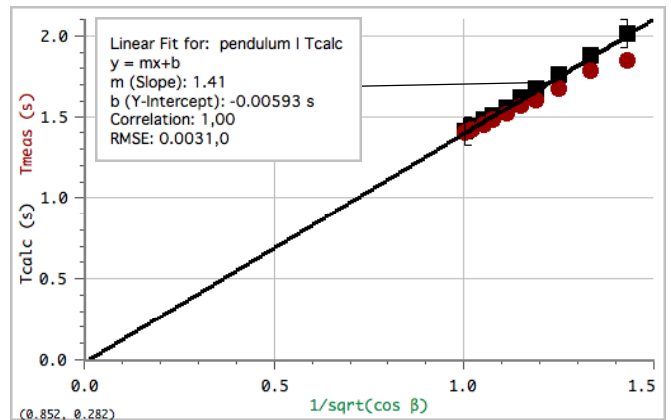


FIGURE 12. Pendulum period vs. $1/\sqrt{\cos \beta}$. Circles: measured periods. Squares: calculated values.

The expected dependence of the measured period on the inverse square root of $\cos \beta$ is substantially confirmed.

The slight systematic difference between the measured periods and the values predicted by the model may be explained by considering that the thin rod is not perfectly rigid: it bends more and more when increasing the tilt angle (due to the mass weight) and this produces an increasing error in the measured tilt angle

X. CONCLUSIONS

We reported an example of use of real time data acquisition studied with the aid of simple numerical simulations. A quite old experiment (the pendulum motion) is refurbished by including the *analysis of both damping and large amplitude oscillations* allowed by the power of modern computers through the joint use of RTL (Real Time Laboratory) and spreadsheet.

Most part of this work was presented by one of the authors (G.T) at the GIREP 2008 conference in Cyprus.

REFERENCES

- [1] Feynmann, R., *The Feynman Lectures on Physics*, (Addison-Wesley, 1963) vol.1 ch. 9-6.
- [2] For the dry friction we follow the nice analysis made by Molina, M. I. in *The Physics Teacher* **42**, 485-487 (2004).
- [3] See LEPLA Project <<http://www.lepla.edu.pl>>; we tried with success also a Vernier rotary sensor (model RMV-BTD), by adding to it the aluminum disc, magnet and brush.
- [4] We tested Texas Instruments graphing calculators as TI89, TI92, TIInspire with CBL interface <<http://ti.education.com>>, and Vernier LabPro interface with LoggerPro software on Windows or Mac OS <<http://www.vernier.com>>, but also the excellent Coach interface <<http://www.cma.science.uva.nl>> and software may be well used.